Journal Name

RSCPublishing

COMMUNICATION

Unprecedented Spin Localisation in a Metal-Metal Bonded Dirhenium Complex†

Cite this: DOI: 10.1039/xoxxoooooox

Yong Yan,[a‡] Joel T. Mague,[a] James P. Donahue[a] and Stephen Sproules*[b]

Received ooth January 2012,
Accepted ooth January 2012

DOI: 10.1039/xoxxoooooox

www.rsc.org/

The molecular and electronic structure of edge-sharing bioctahedral [N(*n*-Bu)$_4$]$_3$[Re$_2$(mnt)$_5$] is reported here. Despite the short intermetal bond length of 2.6654(2) Å with computed bond order of 1.2, the unpaired electron is localised by the asymmetric ligand distribution, as demonstrated by its remarkable EPR spectrum.

The existence of direct metal-to-metal multiple bonds was first demonstrated with the identification of Re-Re double bonds in the structure of $Cs_3[Re_3Cl_{12}]$.[1] This discovery marked the inception of the field of multicenter transition metal chemistry, which expanded inorganic structural and bonding ideas beyond the traditional Wernian motif of a single metal ion surrounded by a set of ligands. Just a year later came the structural characterization of [N(*n*-Bu)$_4$]$_2$[Re$_2$Cl$_8$],[2] a species with an unanticipated short Re-Re distance that was quickly interpreted as being due to a metal-metal quadruple bond. This first recognition of a quadruple bond redefined the bond order (b.o.) ceiling – a value previously seen as being limited at three. Since that time, the body of crystallographically characterized multimetallic complexes with multiply bonded metal atoms has grown rapidly and steadily, the number now being in the thousands and involving all but two elements across groups 5 – 10.[3] The eclipsed arrangement of the square planar opposing $ReCl_4$ units is brought about by the strength of the metal-metal bonds. Each Re^{III} ion has one d orbital ($d_{x^2-y^2}$) Ã bonded to four Cl^- ligands. The remaining four d orbitals form one Ãbond (d_{z^2}-d_{z^2}), two Àbonds (d_{xz}-d_{xz}, d_{yz}-d_{yz}), and a ´ bond (d_{xy}-d_{xy}), giving a b.o. of 4. This ´ bond contributes to stabilizing the D_{4h}-symmetric eclipsed structure. The chemistry of the quadruple bond has been examined in oxidative additions reactions with various small molecules that have led to a plethora of new edge-sharing bioctahedral (ESBO) M_2L_{10} species,[3,4] a commonly encountered motif in molecular and solid state chemistry. The effect upon the Re-Re bond order, now with one d orbital removed from interacting with the other metal by bonding to the new ligands, has been conveniently appraised by X-ray diffraction, or in the absence of suitable crystals, by spectroscopy.

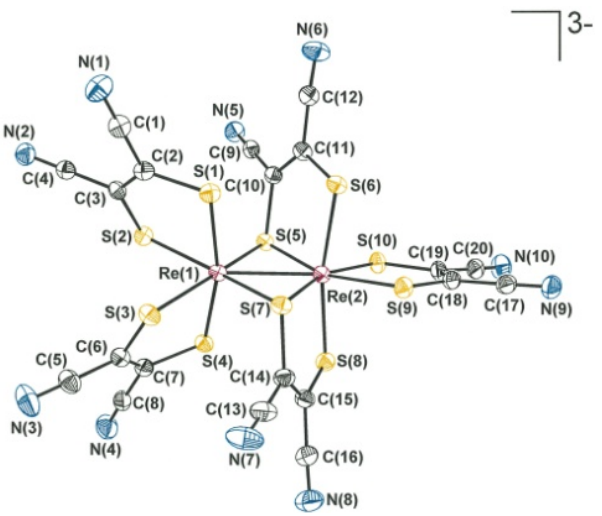

Fig. 1 Structure of the anion in crystals of [N(*n*-Bu)$_4$]$_3$[Re$_2$(mnt)$_5$]·$C_2H_4Cl_2$. Thermal ellipsoids are shown at the 50% probability level. Selected bond lengths (Å): Re(1)−Re(2) 2.6654(2), Re(1)−S(1) 2.3997(9), Re(1)−S(2) 2.4358(9), Re(1)−S(3) 2.4161(9), Re(1)−S(4) 2.3681(9), Re(1)−S(5) 2.4020(9), Re(1)−S(7) 2.3986(9), Re(2)−S(5) 2.3244(8), Re(2)−S(6) 2.3758(9), Re(2)−S(7) 2.3124(9), Re(2)–S(8) 2.3826(9), Re(2)−S(9) 2.4267(9), Re(2)−S(10) 2.4125(9).

With our continuing investigation into dithiolene chemistry of third row transition metals,[5,6,7,8] we revisited the reaction of [N(*n*-Bu)$_4$]$_2$[Re$_2$Cl$_8$] with disodium maleonitriledithiolate, Na_2mnt,[9] with the intent of determining its molecular structure. The original report by Cotton, Oldham and Walton detailed the isolation of an almost black microcrystalline solid, formulated [AsPh$_4$]$_2$[Re$_2$(mnt)$_4$],[9] although the exact geometry and Re-Re bond order had not been definitively established. A reproduction of this reaction by stirring [N(*n*-Bu)$_4$]$_2$[Re$_2$Cl$_8$] and Na_2mnt in dichloromethane at ambient temperature led to the isolation of [N(*n*-Bu)$_4$]$_3$[Re$_2$(mnt)$_5$] in modest

yield (38%). The formation of a mixed-valence $Re^{III,IV}$ species appears to arise from the presence of adventitious dioxygen or oxidation by the solvent, dichloromethane. The same reaction performed under aerobic conditions yielded [N(*n*-Bu)$_4$][ReO(mnt)$_2$],[10] as confirmed by X-ray crystallography (Fig. S1).

Black columns that crystallized in the monoclinic space group $P2_1/c$ showed one $[Re_2(mnt)_5]^{3-}$ anion, three well separated tetrabutylammonium cations and a 1,2-dichloroethane solvent molecule. The dimetallic complex contains a $\{Re_2S_{10}\}$ core with each Re ion possessing approximate octahedral coordination to six sulfur atoms (Fig. 1). This ESBO complex can be viewed as an $[Re^{III}(mnt)_2]^{1-}$ unit (Re(1) in Fig. 1) attached to an octahedral $[Re^{IV}(mnt)_3]^{2-}$ species (Re(2) in Fig. 1) through sulfur atoms in the cis position, with a C_2 axis along the metal-metal vector. This topology has been observed with dirhenium compounds with di- and tri-thiocarbamate ligands[11] and in one example with 4,5-disulfanyl-1,3-dithiole-2-thionate, $(dmit)^{2-}$.[12] The dimensions of the "Re(mnt)$_3$" component are almost identical to $[PPh_4]_2[Re^{IV}(mnt)_3]$, with the average Re(2)–S bond length at 2.3724(9) Å similar to the monometallic species (2.364(1) Å).[8] It is significant that the average Re(1)–S distance is 0.031 Å longer than for Re(2), which leads to a tentative oxidation state assignment of +III for Re(1). The two chelating $(mnt)^{2-}$ ligands about Re(1) exhibit a noticeable distortion along the S···S vector reducing the fold angle to 159° and resemble the corresponding ligands in $[Re^{IV}_2(dmit)_5]^{2-}$.[12] All intraligand bond lengths are consistent with the dianionic form of the ligand. The short intermetal separation of 2.6654(2) Å is indicative of metal-metal bonding. This value sits in the range for structurally characterised ESBO complexes containing a $\{Re_2\}^{7+}$ core: $[Re_2(NCS)_{10}]^{3-}$ (2.613(1) Å),[13] $[Re_2Cl_6(dppm)_2]^{1+}$ (2.682(1) Å; dppm = bis(diphenylphosphino)methane),[14] $[Re_2OCl_3(O_2CCH_2CH_3)_2(PPh_3)_2]$ (2.514(1) Å),[15] $[Re_2OCl_2(pyt)_4]^{1-}$ (2.5491(4) Å; $(pyt)^{1-}$ = pyridine-2-thiolate).[16]

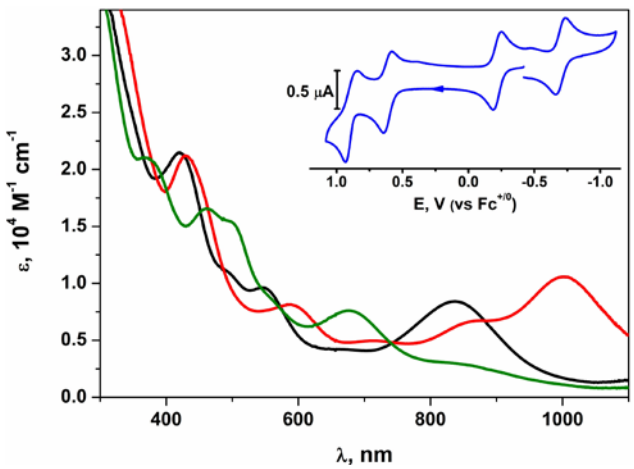

Fig. 2 Electronic spectra of electrochemically generated $[Re_2(mnt)_5]^{2-}$ (red), $[Re_2(mnt)_5]^{3-}$ (black), and $[Re_2(mnt)_5]^{4-}$ (green) species in CH_2Cl_2 (0.10 M [N(*n*-Bu)$_4$]PF$_6$) at -25 °C. Inset shows the cyclic voltammogram taken under the same conditions at 100 mV s^{-1} referenced to the $Fc^{+/0}$ couple.

The redox chemistry of [N(*n*-Bu)$_4$]$_3$[Re$_2$(mnt)$_5$] was probed by electro- and spectroelectrochemistry. The cyclic voltammogram recorded in dichloromethane solution at -25 °C revealed four redox events (Fig. 2 inset): a one-electron reduction at -0.704 V, and three oxidation processes at -0.220, +0.613, and +0.905 V versus $Fc^{+/0}$. By comparison, the corresponding processes for $[Re_2(dmit)_5]^{2-}$ occur at lower potential: -1.20, -0.86, -0.12, and -0.05 V, respectively.[12] The ease of oxidising the latter underscores the stronger À-donation of the $(dmit)^{2-}$ ligand, which results in stabilisation of the dirhenium complex as a dianion rather than as a trianion as in $[Re_2(mnt)_5]^{3-}$. Controlled potential coulometry confirmed the reduction and the first oxidation as fully reversible. Simultaneous measurement of their electronic spectra revealed several isosbestic points during each electrochemical transformation (Figures S2 and S3). The other oxidation waves are not reversible on the timescale of the experiment. In an electrochemical study of the rhenium $(mnt)^{2-}$ species isolated using the original published procedure, McCleverty and co-workers[10] revised the molecular formula as $[Re(mnt)_2]_4^{4-}$ to account for the charge per mole of the complex. Their voltammogram revealed this species was reversibly reduced at -0.70 V and oxidized at -0.29 V. Both of these processes are essentially identical to redox features observed for $[Re_2(mnt)_5]^{3-}$ when corrected for different solvent, electrolyte and reference electrode.[5] It is therefore probable that they had also isolated [N(*n*-Bu)$_4$]$_3$[Re$_2$(mnt)$_5$].[9] Despite the presence of redox-active dithiolene ligands, all redox processes are defined as metal-centred up to +V, following the trend established for tris(dithiolene) complexes.[5,7,8] Therefore, the five-membered electron transfer series is classified as:

$$[Re_2^{V,V}]^0 \underset{-e}{\overset{+e}{\rightleftharpoons}} [Re_2^{IV,V}]^{1-} \underset{-e}{\overset{+e}{\rightleftharpoons}} [Re_2^{IV,IV}]^{2-} \underset{-e}{\overset{+e}{\rightleftharpoons}} [Re_2^{III,IV}]^{3-} \underset{-e}{\overset{+e}{\rightleftharpoons}} [Re_2^{III,III}]^{4-}$$
$$(S = 0) \qquad (S = {}^1/_2) \qquad (S = 0) \qquad (S = {}^1/_2) \qquad (S = 0)$$

The electronic spectra for the three stable members of the series are overlaid in Fig. 2. The parent complex [N(*n*-Bu)$_4$]$_3$[Re$_2$(mnt)$_5$] has a significantly intense (μ = 8400 M^{-1} cm^{-1}) peak at 836 nm. It is interesting to note that the electronic spectral data provided in the original report match our spectrum for [N(*n*-Bu)$_4$]$_3$[Re$_2$(mnt)$_5$].[9] The one-electron reduced tetra-anionic species has a low-energy shoulder at 809 nm and a more prominent band at 675 nm. The spectral profile of the dianionic member of the series is dominated by a peak at 1003 nm (10 600 M^{-1} cm^{-1}) with a shoulder at 876 nm. The prominent low energy band for each complex is too intense to be due to an excitation between molecular orbitals (MO) of the dirhenium unit and is most likely ligand-to-metal charge transfer from filled À MOs to metal-based MOs of Àsymmetry, such as the vacant À* MO in each member of the series (vide infra).

With an uneven number of valence electrons, the $S = {}^1/_2$ ground state of [N(*n*-Bu)$_4$]$_3$[Re$_2$(mnt)$_5$] is conveniently probed by EPR spectroscopy. The spectrum presented in Fig. 3 is the most extraordinary of any known dirhenium complex.[17,18] No signal was observed in room temperature or chilled solution. The profile is dominated by six hyperfine lines rather than an anticipated 11-line pattern arising from two Re ions with the ^{185,187}Re isotopes of nuclear spin $I = {}^5/_2$ (100% abundant). This outcome can only arise if the unpaired electron is *localised* on one Re ion, and despite the metal-metal bond, no coupling is observed with the second Re ion. The spectrum was best reproduced with g = (1.878, 1.989, 2.028) and A = (290, 330, 45) × 10^{-4} cm^{-1}, which are similar in magnitude to the only other simulated spectrum of a paramagnetic dirhenium species possessing a $\{Re_2\}^{7+}$ core, $[Re_2(hpp)_4Cl_2]^{1+}$.[18] Successful simulation required the sparingly utilised quadrupolar term (**P**). Spectacularly large quadrupolar couplings were recently found in the EPR spectra of neutral tris(dithiolene)rhenium compounds and their two-electron reduced complex dianions.[7] Similar features can be seen in the spectrum shown in Fig. 3, namely an uneven spacing of the six hyperfine lines and weak quadrupole-allowed transitions in the low field region of the spectrum. The best fit emerged for a rhombic **P** tensor: P = (24, 16, -40) × 10^{-4} cm^{-1},[19] which is parameterised by $P = [P_{zz} - (P_{xx} + P_{yy})/2]/3 = 20 \times 10^{-4}$ cm^{-1} and rhombicity, · = $(P_{xx} - P_{yy})/2 = 4 \times 10^{-4}$ cm^{-1}. This quadrupolar coupling is similar to $[Re^{IV}(bdt)_3]^{2-}$ (bdt^{2-} = benzene-1,2-dithiolate),[7] and sits amongst those determined for a variety of Re^{VI} compounds.[20]

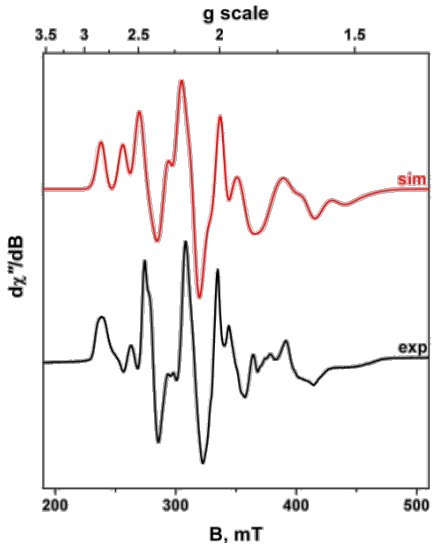

Fig. 3 X-band EPR spectrum of $[N(n\text{-}Bu)_4]_3[Re_2(mnt)_5]$ recorded in CH_2Cl_2/THF solution at 20 K. The simulation is shown in red with the experimental spectrum in black (conditions: frequency, 9.4365 GHz; power, 0.063 mW; modulation, 1.5 mT).

The **g** and **A** matrices, and **P** tensor were all assumed to be coaxial in this simulation. It should be noted that this may not be a unique solution, and additional data are required to resolve the potentially complicated tensor orientations inherent to low symmetry complexes. A mixture of *g*- and *A*-strain was employed to model the spectral linewidth, which presumably stems from structural heterogeneity in the frozen glass. Based on the homogeneous linewidth, coupling to the second Re ion can be limited to a maximum value of 20×10^{-4} cm^{-1}. However, there is no evidence to support the existence of this interaction.

The electronic structure for this electron transfer series has been determined by DFT calculations. The optimized structure for the trianion has average Re(1)–S and Re(2)–S bond lengths of 2.422 and 2.395 Å, respectively (Table S2). These values are ~0.02 Å longer than the experimental data, which is typical of the B3LYP functional. The Re–Re distance at 2.736 Å is substantially overestimated (by 0.07 Å), and the two terminal dithiolene ligands on Re(1) retain a noticeable fold angle of ~170° (cf. 159° experimentally). In a simple ligand field description, the available d orbitals for each metal ion in an ESBO form three metal-metal bonds:[4] one Ã bond between $d_{x^2-y^2}$ orbitals; one À bond between d_{xz} orbitals, and a ´ bond between d_{yz} orbitals, where the *x*-axis is parallel to the metal-metal vector (Fig. 4b). The MO manifold calculated for $[Re_2(mnt)_5]^{3-}$ shows a bona fide Ã bond. However, the strong interaction between the À orbital of the single terminal $(mnt)^{2-}$ ligand of Re(2) stabilises the d orbital manifold and disrupts the overlap with the corresponding orbital on Re(1). The consequence is attenuation of the Re-Re À bond and complete destruction of the ´ bond, leading to an unambiguous assignment of a d^3 electron count for Re(2) and d^4 for Re(1). An identical solution resulted from broken symmetry calculations, such that the electronic structure cannot be viewed as the consequence of strong antiferromagnetic coupling between $S = 1$ and $S = {}^1/_2$ ions, which is highly unlikely for 5d metals. The Mulliken spin population analysis reveals one unpaired electron at Re(1) with a minor polarization of the metal-metal bond depositing some spin density at the second ion (Fig. 4a). The structural, spectroscopic and computational data support the assignment as a Class I valence localized $\{Re^{III}Re^{IV}\}$ compound.[21] The calculated bond order (Löwdin) of 1.2 is in keeping with the experimental intermetal bond distance when compared to similar $\{Re_2\}^{7+}$ units with b.o. ~ 1.5 (vide supra). The molecular and electronic structures of the di- and tetra-anionic members of the electron transfer series were similarly computed (Figures S5-S8). Both are diamagnetic as shown by the absence of an EPR signal on samples generated by bulk electrolysis.

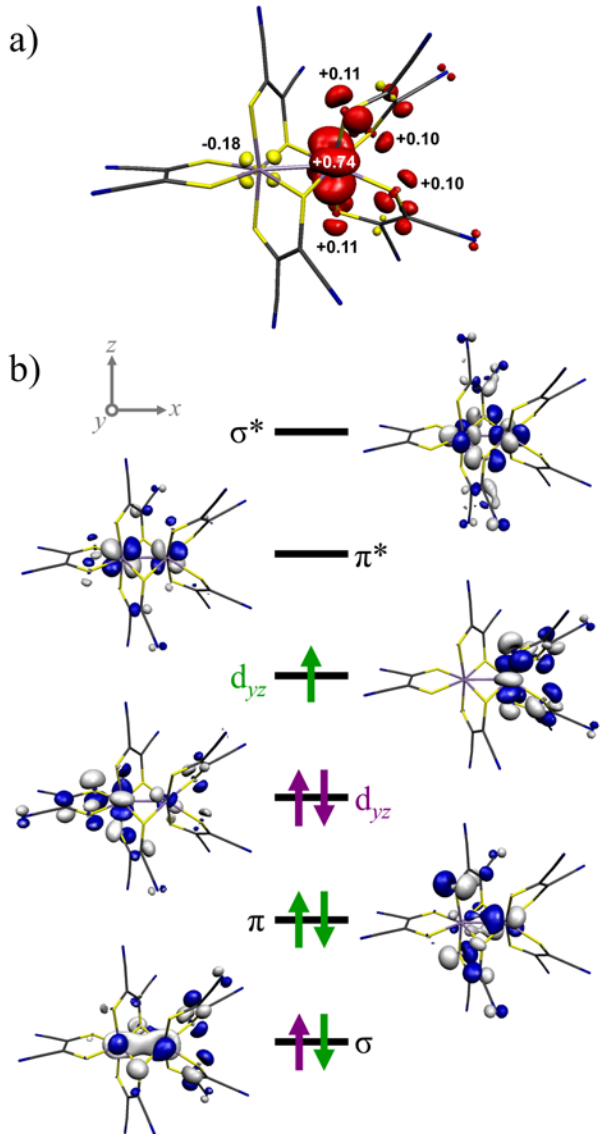

Fig. 4 (a) Mulliken spin population analysis for $[Re_2(mnt)_5]^{3-}$ from spin unrestricted DFT calculations (red: ±-spin, yellow: ²-spin). (b) Qualitative MO scheme depicting the ordering of the Kohn-Sham orbitals (²-spin) for the $\{Re_2\}^{7+}$ unit in $[Re_2(mnt)_5]^{3-}$.

The intermetal separation diminishes with decreasing metal oxidation state (Table S2). One-electron oxidation to $[Re_2(mnt)_5]^{2-}$ gives a Re-Re bond distance of 2.794 Å. After correcting for the DFT overestimation of 0.07 Å (vide supra), this bond length is similar to the 2.721(2) Å Re-Re distance in $[Re_2(dmit)_5]^{2-}$, which also possesses a C_2 symmetric $\{Re_2\}^{8+}$ core.[12] The one-electron reduced species has an intermetal separation of 2.705 Å from a starting position of 2.736 Å in $[Re_2(mnt)_5]^{3-}$. This distance is still longer than the intermetal separation of 2.573(2) Å in $[Re_2(\mu\text{-}S_3CNMe_2)_2(S_2CNMe_2)_3]^{1+}$ with a C_2 symmetric $\{Re_2\}^{6+}$ core, which stems from the monoanionic charge and reduced bite angle of its di- and tri-thiocarbamate ligands.[11] The short distance results from a better energy match between adjacent d_{xz} orbitals strengthening the

Re-Re À in the tetra-anionic complex (Fig. S8). The $(mnt)^{2-}$ Å*-d_{yz} interaction stabilises this orbital relative to the Re-Re Àbonding MO. In contrast, the Re-Re À bond is completely absent in $[Re_2(mnt)_5]^{2-}$ (Fig. S7), where the high positive charge on adjacent ions leads to an elongation of the Re-Re bond, as reflected in a computed bond order approaching unity (Table S2).

The valence localised electronic structure of $[Re_2(mnt)_5]^{3-}$ is driven by strong metal-ligand bonds that override the intermetal interaction, unlike in the archetypal octachlorodirhenate.[2] The highly covalent bonding between soft sulfur-donor dithiolenes and transition metal ions renders these chelates unsuitable for forming paddle-wheel or lantern structures where higher bond orders would be anticipated. A detailed understanding of the inherent physical properties of third row metals such as rhenium will enable their exploitation in new magnetic and spintronic materials. The work is supported by PRF grant 45685-G3 and NSF grant CHE-0845829, and start-up funds from the University of Glasgow.

Notes and references

[a] Department of Chemistry, Tulane University, 6400 Freret Street, New Orleans, LA 70118-5698, USA.

[b] WestCHEM, School of Chemistry, University of Glasgow, Glasgow G12 8QQ, UK. E-mail: stephen.sproules@glasgow.ac.uk

† Electronic Supplementary Information (ESI) available: Experimental and crystallographic details (CCDC 1024622 and 1024623), spectroelectrochemical titrations, and computational data. See DOI: 10.1039/c000000x/

‡ Present address: National Renewable Energy Lab, Golden, CO 80401, USA.

1. J. A. Bertrand, F. A. Cotton and W. A. Dollase, *Inorg. Chem.*, 1963, **2**, 1166.
2. F. A. Cotton, N. F. Curtis, C. B. Harris, B. F. G. Johnson, S. J. Lippard, J. T. Mague, W. R. Robinson and J. S. Wood, *Science*, 1964, **145**, 1305.
3. F. A. Cotton, C. A. Murillo and R. A. Walton, *Multiple Bonds between Metal Atoms*, Springer, New York, 2005.
4. F. A. Cotton, *Polyhedron*, 1987, **6**, 667.
5. S. Sproules, *Prog. Inorg. Chem.*, 2014, **58**, 1.
6. (a) S. Sproules, P. Banerjee, T. Weyhermüller, Y. Yan, J. P. Donahue and K. Wieghardt, *Inorg. Chem.*, 2011, **50**, 7106. (b) Y. Yan, P. Chandrasekaran, J. T. Mague, S. DeBeer, S. Sproules and J. P. Donahue, *Inorg. Chem.*, 2012, **51**, 346. (c) Y. Yan, C. Keating, P. Chandrasekaran, U. Jayarathne, J. T. Mague, S. DeBeer, K. M. Lancaster, S. Sproules, I. V. Rubtsov and J. P. Donahue, *Inorg. Chem.*, 2013, **52**, 6743.
7. S. Sproules, F. L. Benedito, E. Bill, T. Weyhermüller, S. DeBeer George and K. Wieghardt, *Inorg. Chem.*, 2009, **48**, 10926.
8. S. Sproules, T. Weyhermüller, R. Goddard and K. Wieghardt, *Inorg. Chem.*, 2011, **50**, 12623.
9. F. A. Cotton, C. Oldham and R. A. Walton, *Inorg. Chem.*, 1967, **6**, 214.
10. N. G. Connelly, C. J. Jones and J. A. McCleverty, *J. Chem. Soc. A*, 1971, 712.
11. (a) H. H. Murray, L. Wei, S. E. Sherman, M. A. Greaney, K. A. Eriksen, B. Carstensen, T. R. Halbert and E. I. Stiefel, *Inorg. Chem.*, 1995, **34**, 841. (b) L. Wei, T. R. Halbert, H. H. Murray, III and E. I. Stiefel, *J. Am. Chem. Soc.*, 1990, **112**, 6431.
12. G. Matsubayashi, T. Maikawa, H. Tamura, M. Nakano and R. Arakawa, *J. Chem. Soc., Dalton Trans.*, 1996, 1539.
13. F. A. Cotton, A. Davison, W. H. Ilsley and H. S. Trop, *Inorg. Chem.*, 1979, **18**, 2719.
14. K. R. Dunbar, D. Powell and R. A. Walton, *Chem. Commun.*, 1985, 114.
15. F. A. Cotton, R. Eiss and B. M. Foxman, *Inorg. Chem.*, 1969, **8**, 950.
16. K. Umakoshi, N. Misasa, C. Ohtsu, T. Kojima, M. Sokolov, M. Wakeshima, Y. Hinatsu and M. Onishi, *Angew. Chem. Int. Ed.*, 2005, **44**, 720.
17. (a) P. Brant, D. J. Salmon and R. A. Walton, *J. Am. Chem. Soc.*, 1978, **100**, 4424. (b) M. T. Costello, D. R. Derringer, P. E. Fanwick, A. C. Price, M. I. Rivera, E. Scheiber, E. W. Siurek, III and R. A. Walton, *Polyhedron*, 1990, **9**, 573. (c) F. A. Cotton and E. Pedersen, *J. Am. Chem. Soc.*, 1975, **97**, 303. (d) F. A. Cotton, A. C. Price and K. Vidyasagar, *Inorg. Chem.*, 1990, **29**, 5143. (e) V. Srinivasan and R. A. Walton, *Inorg. Chem.*, 1980, **19**, 1635.
18. F. A. Cotton, N. S. Dalal, P. Huang, S. A. Ibragimov, C. A. Murillo, P. M. B. Piccoli, C. M. Ramsey, A. J. Schultz, X. Wang and Q. Zhao, *Inorg. Chem.*, 2007, **46**, 1718.
19. The sign of the **P** tensor components is not known, so we assume *z* to be negative.
20. (a) A. H. Al-Mowali and A. L. Porte, *J. Chem. Soc., Dalton Trans.*, 1975, 50. (b) L. V. Borisova, A. S. Borodkov, A. A. Grechnikov, E. A. Ugolkova and V. V. Minin, *Russ. J. Inorg. Chem.*, 2013, **58**, 940. (c) J. C. Brewer, H. H. Thorp, K. M. Slagle, G. W. Brudvig and H. B. Gray, *J. Am. Chem. Soc.*, 1991, **113**, 3171. (d) R. Gazzinelli, O. F. Schirmer and V. Wittwer, *J. Phys. C: Solid State Phys.*, 1977, **10**, 889. (e) J. F. Gibson, G. M. Lack, K. Mertis and G. Wilkinson, *J. Chem. Soc., Dalton Trans.*, 1976, 1492. (f) J. F. Gibson, K. Mertis and G. Wilkinson, *J. Chem. Soc., Dalton Trans.*, 1975, 1093. (g) J. H. Holloway and J. B. Raynor, *J. Chem. Soc., Dalton Trans.*, 1975, 737. (h) G. M. Lack and J. F. Gibson, *J. Mol. Struct.*, 1978, **46**, 299. (i) A. Venturelli, M. J. Nilges, A. Smirnov, R. L. Belford and L. C. Francesconi, *J. Chem. Soc., Dalton Trans.*, 1999, 301. (j) A. Voigt, U. Abram, R. Böttcher, U. Richter, J. Reinhold and R. Kirmse, *Chem. Phys.*, 2000, **253**, 171.
21. M. B. Robin and P. Day, *Adv. Inorg. Chem. Radiochem.*, 1967, **10**, 247.

Electronic Supplementary Information

Unprecedented Spin Localisation in a Metal-Metal Bonded Dirhenium Complex

Yong Yan,[a] Joel T. Mague,[a] James P. Donahue,[a] and Stephen Sproules*[b]

[a] Department of Chemistry, Tulane University, 6400 Freret Street, New Orleans, LA 70118-5698, United States

[b] WestCHEM, School of Chemistry, University of Glasgow, Glasgow G12 8QQ, UK

Experimental Section

Synthesis. The disodium salt of maleontriledithiolate, Na_2mnt, was prepared following the literature procedure.[1] $[N(n\text{-}Bu)_4]_2[Re_2Cl_8]$ was purchased from Aldrich. Solvents either were dried with a system of drying columns from the Glass Contour Company (CH_2Cl_2, Et_2O, hexanes) or freshly distilled according to standard procedures (1,2-$C_2H_4Cl_2$, ^{t}BuOMe).[2]

$[N(n\text{-}Bu)_4]_3[Re_2(mnt)_5]$. Blue-green $[N(n\text{-}Bu)_4]_2[Re_2Cl_8]$ (77mg; 0.067 mmol) and pale yellow Na_2(mnt) (75mg, 0.402 mmol) were combined with dichloromethane (25 mL) in a 50 mL Schlenk flask charged with a magnetic bar under a N_2 atmosphere. The stirred reaction mixture gradually changed color from green to brownish-yellow and then dark brown. After 6 h, the reaction solution was filtered through Celite, and the solvent was subsequently removed under vacuum. The residue was washed with hexanes (3 × 5 mL) followed by diethyl ether (3 × 5 mL) and then was dried under vacuum. Yield: 39 mg (38%). Diffraction quality black needles were grown by slow diffusion of *t*-BuOMe into a 1,2-dichloroethane solution of the complex.

Anal. Calcd for $C_{70}H_{112}Cl_2N_{13}S_{10}Re_2$: C, 44.25; H, 5.94; N 9.58; S, 16.87. Found: C, 44.80; H, 5.88; N 9.93; S, 15.65%. IR (KBr, cm^{-1}): ½(CN) 2208 s, 2194 m.

The same reaction performed in an aerobic environment yielded a product identified as $[N(n\text{-}Bu)_4][ReO(mnt)_2]$.[3]

X-ray Crystallographic Data Collection and Structure Refinement. Diffraction quality crystals of $[N(n\text{-}Bu)_4]_3[Re_2(mnt)_5]\cdot C_2H_4Cl_2$ as black needles were obtained by slow diffusion of *t*-BuOMe vapour into a 1,2-dichloroethane solution under a N_2 atmosphere. When the preparation of $[N(n\text{-}Bu)_4]_3[Re_2(mnt)_5]$ was attempted in the open atmosphere, the product isolated was [N(*n*-

Bu)$_4$][ReO(mnt)$_2$], orange block crystals of which were obtained by the diffusion of Et_2O vapor into a MeCN solution. The crystals were coated with paratone oil and mounted on the end of a nylon loop attached to the end of the goniometer. Data were collected with a Bruker SMART APEX CCD diffractometer equipped with a Kryoflex attachment supplying a nitrogen stream at 100 K. Full spheres of data were obtained by collecting three sets of 400 frames in *É* (0.5º/scan), collected at *Æ*= 0.00, 90.00 and 180.00° followed by two sets of 800 frames in *Æ*(0.45°/scan) collected with *É* constant at -30.00 and 210.00°. Frames times of 20 and 10 seconds/frame were used for [N(*n*-Bu)$_4$]$_3$[Re$_2$(mnt)$_5$]·ClCH$_2$CH$_2$Cl and [N(*n*-Bu)$_4$][ReO(mnt)$_2$], respectively. Diffraction data were collected under control of one of the *APEX2*[4] software packages. Raw data were reduced to F^2 values using the *SAINT*[5] software, and a global refinement of unit cell parameters was performed using ~9900 selected reflections from the full data set. Data for [N(*n*-Bu)$_4$]$_3$[Re$_2$(mnt)$_5$]·$C_2H_4Cl_2$ were corrected for absorption on the basis of multiple measurements of symmetry equivalent reflections with the use of *SADABS*,[6] while the correction for [N(*n*-Bu)$_4$][ReO(mnt)$_2$] was performed analytically using the SCALE routine within *APEX2*.[4] Structure solutions were obtained by direct or Patterson methods using *SHELXS*,[7] while refinements were accomplished by full-matrix least-squares procedures using *SHELXL*.[8] Both the *SHELXS* and *SHELXL* programs are incorporated into the *SHELXTL*[9] and *APEX2* software suites.

The structure refinements were routine except that one of the *n*-butyl groups of one of the [N(*n*-Bu)$_4$]$^+$ cations in [N(*n*-Bu)$_4$]$_3$[Re$_2$(mnt)$_5$]·$C_2H_4Cl_2$ revealed some disorder. Three of the four carbon atoms of one *n*-butyl group were disordered over two positions and refined with a 65:35 occupancy ratio subject to restraints that imposed a geometry similar to that displayed by the other *n*-butyl groups of the cation. All hydrogen atoms were added in calculated positions (C−H = 0.98–0.99 Å) and included as riding contributions with isotropic displacement parameters tied to those of the carbon atoms to which they were attached. All images were created with the use of *XP*, which also is part of the *SHELXTL*

package.[9] All structures were checked for overlooked symmetry and other errors by the checkCIF service provided by the International Union of Crystallography.[10] Final unit cell data and refinement statistics are collected in Table S1.

Physical Methods. Cyclic voltammogrammetry and coulometric measurements were performed with and EG&G potentiostat/galvanostat. Elemental analyses were performed by Midwest Microlab, LLC of Indianapolis, IN. Electronic absorption spectra were recorded on a Hewlett-Packard 8453 diode-array spectrophotometer (range 200 – 1100 nm). The X-band EPR spectrum was recorded on a Bruker ELEXSYS E500 spectrometer and simulated using the simulation package XSOPHE.[11] The spectra were simulated using the spin-Hamiltonian:

$$\hat{H} = \mu_B \vec{B} \cdot g \cdot \hat{\vec{S}} + \hat{\vec{S}} \cdot A \cdot \hat{\vec{I}} + \hat{\vec{I}} \cdot P \cdot \hat{\vec{I}}$$

$$\hat{H} = \mu_B \vec{B} \cdot g \cdot \hat{\vec{S}} + \hat{\vec{S}} \cdot A \cdot \hat{\vec{I}} + P_{zz}[3\hat{\vec{I}}_z^2 - I(I+1)] + (P_{xx} - P_{yy})(\hat{\vec{I}}_x^2 - \hat{\vec{I}}_y^2)$$

where μ_B is the electronic Bohr magneton, B is the applied magnetic field, g and A are the electronic g matrix and ^{185,187}Re nuclear hyperfine matrix, respectively, and P_{ii} ($i = x, y, z$) are the principal values of the nuclear quadrupole interaction tensor P, defined by:

$$P_{ii} = \frac{eQq_{ii}}{2I(2I-1)}$$

and

$$q_{ii} = \frac{\partial^2 V}{\partial i^2}$$

where e is the electronic charge, Q is the quadrupole moment of the ^{185,187}Re nuclei (2.33 and 2.22 × 10^{-24} cm^2, respectively) and q_{ii} are the principal values of the electric field gradient at the nucleus. The P tensor is traceless, and its principal components are parameterized by $P = [P_{zz} – (P_{xx} + P_{yy})/2]/3$ and a rhombic term, $\cdot = (P_{xx} – P_{yy})/2$.

Calculations. All calculations in this work were performed with the electronic structure program ORCA.[12] Geometry optimizations were carried out using the B3LYP functional.[13] A segmented all-electron relativistically contracted basis set of triple-¶-quality (def2-TZVP) was used all atoms.[14] A scalar relativistic correction was applied using the zeroth-order regular approximation (ZORA) method.[15] In the context of ZORA, a one center approximation has been shown to introduce only minor errors to the final geometries. Auxiliary basis sets for all complexes used to expand the electron density in the calculations were chosen to match the orbital basis. The self-consistent field (SCF) calculations were tightly converged (1×10^{-8} E_h in energy, 1×10^{-7} E_h in the density change, and 1×10^{-7} in the maximum element of the DIIS error vector). The geometry search for all complexes was carried out in redundant internal coordinates without imposing geometry constraints. Single point energies were run using the same conditions detailed for the optimization. Kohn-Sham orbitals and density plots were constructed using the program Molekel.[16]

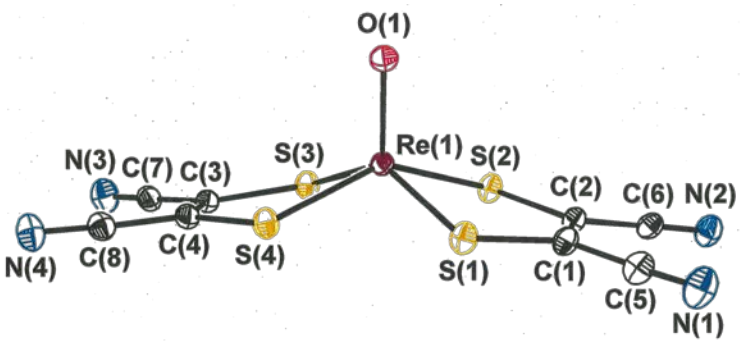

Fig. S1 Structure of the anion in crystals of $[N(n\text{-}Bu)_4][ReO(mnt)_2]$. Thermal ellipsoids are shown at the 50% probability level. Selected bond lengths (Å): Re(1)–O(1) 1.688(1), Re(1)–S(1) 2.3180(4), Re(1)–S(2) 2.3136(4), Re(1)–S(3) 2.3229(4), Re(1)–S4 2.3263(4).

Table S1 Crystallographic Data

compound	$[N(n\text{-}Bu)_4]_3[Re_2(mnt)_5]$	$[N(n\text{-}Bu)_4][ReO(mnt)_2]$
solvent	$C_2H_4Cl_2$	none
formula	$C_{70}H_{112}Cl_2N_{13}S_{10}Re_2$	$C_{24}H_{36}N_5OS_4Re$
fw	1899.63	725.02
T, K	100	100
», Å	0.71073	0.71073
2¸ range, deg	4.00 – 55.88	5.11 – 55.99
crystal system	monoclinic	triclinic
space group	$P2_1/c$	$P\bar{1}$
a, Å	27.314(2)	11.5743(8)
b, Å	11.0154(7)	11.7501(8)
c, Å	29.688(2)	12.5007(8)
±, deg	90	86.489(1)
², deg	104.371(1)	86.473(1)
³, deg	90	60.987(1)
V, Å^3	8653(1)	1483(2)
Z	4	2
Á, g cm^{-3}	1.458	1.623
µ, mm^{-1}	3.144	4.403
crystal size	0.10 × 0.13 × 0.18	0.21 × 0.23 × 0.27
color, habit	black column	orange block
limiting indices, *h*	-35 < *h* < 35	-15 < *h* < 15
limiting indices, *k*	-14 < *k* < 14	-15 < *k* < 15
limiting indices, *l*	-39 < *l* < 39	-16 < *l* < 16
reflections collected	146858	25755
independent data	20740	7092
restraints	6	0
parameters refined	895	321
GoF[a]	1.067	1.082
R1,[b,c] wR2[d,c]	0.0331, 0.0668	0.0142, 0.0358
R1,[b,e] wR2[d,e]	0.0456, 0.0714	0.0145, 0.0360
largest diff. peak, e Å^{-3}	1.331	0.814
largest diff. hole, e Å^{-3}	-1.513	-0.733

[a] GoF = $\{£[w(F_o^2 \bullet F_c^2)^2]/(n \bullet p)\}^{1/2}$, where *n* = number of reflections and *p* is the total number of parameters refined. [b] R1 = $£||F_o| \bullet |F_c||/£|F_o|$. [c] R indices for data cut off at $I > 2Ã(I)$. [d] *w*R2 = $\{£[w(F_o^2 \bullet F_c^2)^2]/£[w(F_o^2)^2]\}^{1/2}$, where $w = 1/[Ã^2(F_o^2) + (aP)^2 + bP]$, $P = (F_o^2 + 2F_c^2)/3$. [e] R indices for all data.

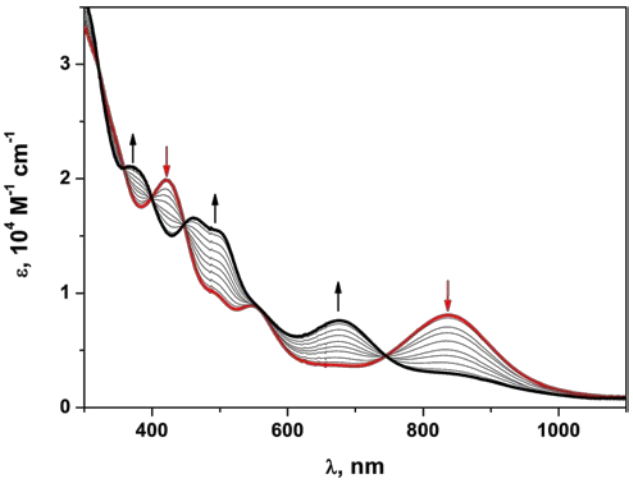

Fig. S2 Electronic spectral titration for the electrochemical reduction of $[Re_2(mnt)_5]^{3-}$ (red) to $[Re_2(mnt)_5]^{4-}$ (black) recorded in CH_2Cl_2 (0.10 M $[N(n\text{-}Bu)_4]PF_6$) at -25 °C.

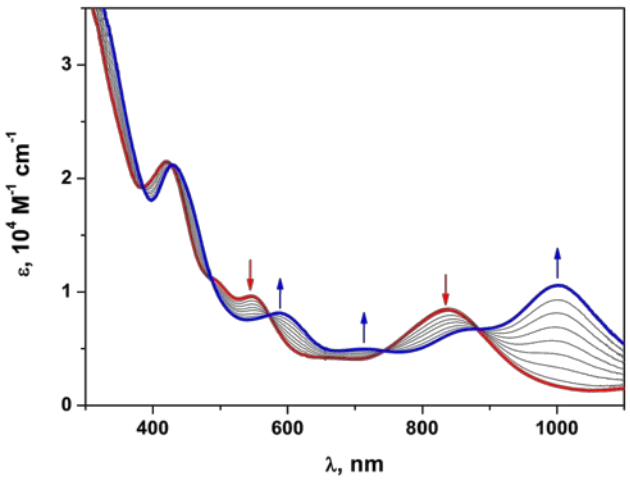

Fig. S3 Electronic spectral titration for the electrochemical oxidation of $[Re_2(mnt)_5]^{3-}$ (red) to $[Re_2(mnt)_5]^{2-}$ (blue) recorded in CH_2Cl_2 (0.10 M $[N(n\text{-}Bu)_4]PF_6$) at -25 °C.

Table S2 Comparison of calculated and experimental (in parentheses) metric parameters (Å)

	$[Re_2(mnt)_5]^{2-}$	$[Re_2(mnt)_5]^{3-}$		$[Re_2(mnt)_5]^{4-}$
Re(1)–Re(2)	2.798	2.736	(2.6654(2))	2.705
b.o. (Löwdin)	1.05	1.20	(1.28)	1.33
$Re(1)–S_{av}$	2.410	2.422	(2.4030(9))	2.422
$Re(2)–S_{av}$	2.389	2.395	(2.3724(9))	2.402

Table S3 Geometry-optimised coordinates for $[Re_2(mnt)_5]^{3-}$

Re	2.788343	-0.014623	0.022845
Re	0.052730	-0.010139	-0.003463
S	4.584737	-1.527025	-0.658037
S	3.076545	0.917845	-2.155402
S	4.581139	1.484662	0.739508
S	3.027620	-0.949318	2.206401
S	-1.756764	-1.646611	0.119782
S	-1.750871	1.628922	-0.166321
S	-0.175163	-0.056863	2.385682
S	1.339736	1.921537	0.311364
S	-0.126764	0.035514	-2.398497
S	1.339320	-1.945896	-0.292601
N	7.199692	-2.073259	-3.203199
N	5.312791	1.094507	-5.095582
N	7.159776	2.001508	3.328242
N	5.215586	-1.154532	5.181055
N	-5.417476	-2.061410	0.115264
N	-5.409876	2.049059	-0.250541
N	0.304830	1.933138	5.451179
N	2.239378	4.543857	2.790857
N	0.405868	-1.961622	-5.451234
N	2.273410	-4.576956	-2.750360
C	5.131455	-0.896913	-2.185313
C	4.500690	0.160121	-2.824716
C	5.097703	0.846481	2.274164
C	4.447377	-0.206525	2.900530
C	-3.219175	-0.699683	0.017430
C	-3.216974	0.683800	-0.098551
C	0.533523	1.431428	2.919701
C	1.192447	2.300859	2.066682
C	0.585010	-1.456542	-2.916294
C	1.223907	-2.327739	-2.049783
C	6.263685	-1.532674	-2.756564
C	4.957148	0.659794	-4.069286
C	6.226277	1.470460	2.865148
C	4.879530	-0.713708	4.150775
C	-4.432468	-1.430645	0.072527
C	-4.427532	1.416241	-0.183484
C	0.423551	1.717321	4.309131
C	1.764170	3.517556	2.484983
C	0.499958	-1.745816	-4.306914
C	1.796850	-3.548250	-2.454886

Table S4 Geometry-optimised coordinates for $[Re_2(mnt)_5]^{2-}$

Re	2.766958	-0.011590	0.024479
Re	-0.031064	-0.006211	-0.004585
S	4.500028	-1.497056	-0.691023
S	2.975126	0.888956	-2.148870
S	4.491710	1.462282	0.780543
S	2.930036	-0.923023	2.199488
S	-1.824127	-1.610641	0.197712
S	-1.814333	1.601924	-0.249490
S	-0.177561	0.023874	2.394289
S	1.260474	1.940189	0.234853
S	-0.128684	-0.044179	-2.408217
S	1.257414	-1.958433	-0.213695
N	7.382560	-1.708264	-2.988814
N	5.476465	1.504667	-4.817454
N	7.346960	1.631802	3.116210
N	5.396830	-1.582457	4.891625
N	-5.483320	-2.052368	0.233484
N	-5.468839	2.054357	-0.381224
N	0.346169	2.121986	5.382053
N	2.208320	4.648298	2.584956
N	0.437788	-2.164389	-5.374534
N	2.234358	-4.682004	-2.533849
C	5.187164	-0.695885	-2.064142
C	4.544607	0.366868	-2.690252
C	5.155879	0.644009	2.155525
C	4.496701	-0.418410	2.764864
C	-3.291335	-0.689980	0.051170
C	-3.287432	0.684349	-0.140630
C	0.510661	1.539695	2.862959
C	1.140438	2.383207	1.964050
C	0.558807	-1.565791	-2.856654
C	1.167774	-2.408386	-1.942517
C	6.390598	-1.245371	-2.582913
C	5.066169	0.978403	-3.858657
C	6.356860	1.179616	2.693923
C	4.999705	-1.044568	3.933724
C	-4.500637	-1.424572	0.152254
C	-4.491865	1.421640	-0.273505
C	0.433046	1.870757	4.245567
C	1.720696	3.617423	2.323332
C	0.503349	-1.905215	-4.238430
C	1.747267	-3.647650	-2.285387

Table S5 Geometry-optimised coordinates for $[Re_2(mnt)_5]^{4-}$

Re	2.888080	-0.014754	0.022534
Re	0.183097	-0.014675	-0.002494
S	4.719728	-1.566765	-0.553504
S	3.287670	0.851638	-2.169342
S	4.711969	1.532159	0.636238
S	3.243180	-0.884126	2.221797
S	-1.640179	-1.673103	-0.046253
S	-1.639935	1.645379	0.003860
S	-0.115146	-0.262809	2.364847
S	1.473952	1.878192	0.480433
S	-0.069583	0.234164	-2.375093
S	1.481870	-1.907733	-0.461254
N	6.883675	-2.739227	-3.311303
N	4.996409	0.306559	-5.408488
N	6.835882	2.685548	3.434152
N	4.902471	-0.361420	5.488168
N	-5.301411	-2.068274	-0.100909
N	-5.304319	2.037205	-0.024164
N	0.269212	1.480431	5.589232
N	2.202153	4.338118	3.188278
N	0.387265	-1.494055	-5.594872
N	2.245245	-4.375658	-3.151971
C	5.051143	-1.258389	-2.243393
C	4.429234	-0.233712	-2.944420
C	5.014450	1.217294	2.330647
C	4.376641	0.193357	3.018074
C	-3.099590	-0.709257	-0.052502
C	-3.099499	0.682155	-0.022726
C	0.586247	1.178748	3.035908
C	1.252368	2.123297	2.273382
C	0.643529	-1.207757	-3.032858
C	1.292786	-2.153757	-2.257755
C	6.050396	-2.059072	-2.845978
C	4.754564	0.048688	-4.290875
C	6.007555	2.010712	2.952431
C	4.678192	-0.094563	4.368995
C	-4.314911	-1.435581	-0.078207
C	-4.315170	1.408291	-0.024419
C	0.434434	1.351384	4.438306
C	1.770411	3.317706	2.800605
C	0.519242	-1.379167	-4.438160
C	1.818412	-3.349312	-2.774731

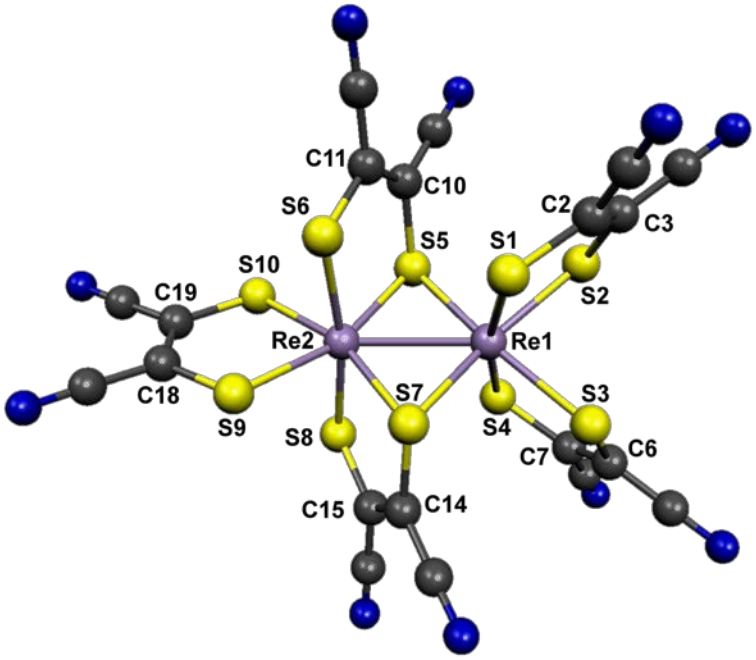

Fig. S4 Geometry-optimised structure of $[Re_2(mnt)_5]^{3-}$

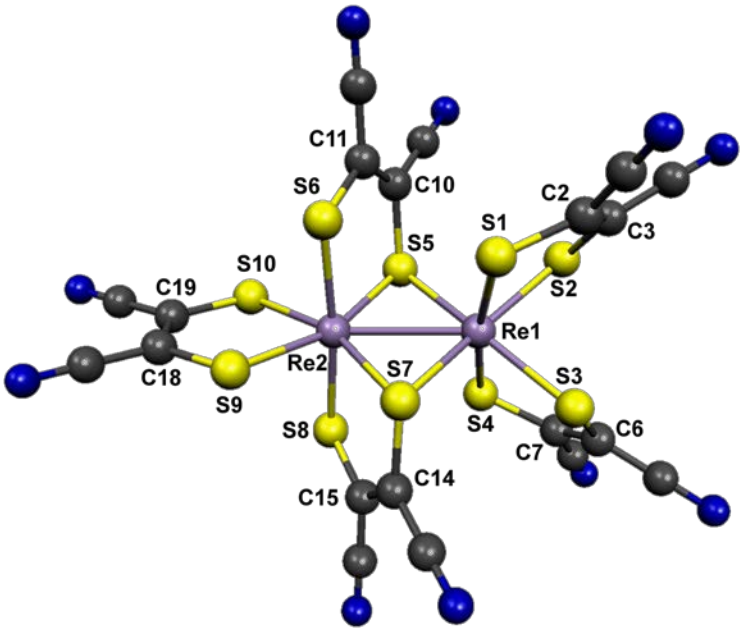

Fig. S5 Geometry-optimised structure of $[Re_2(mnt)_5]^{2-}$

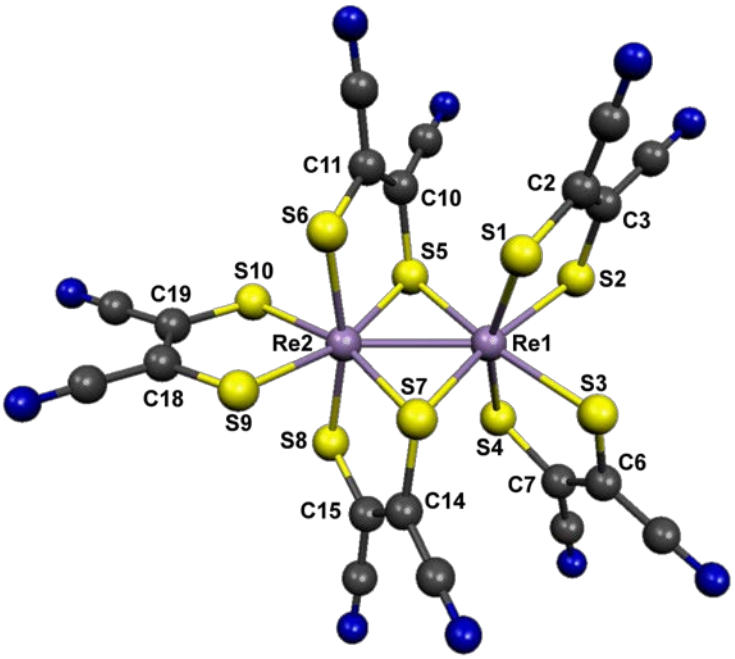

Fig. S6 Geometry-optimised structure of $[Re_2(mnt)_5]^{4-}$

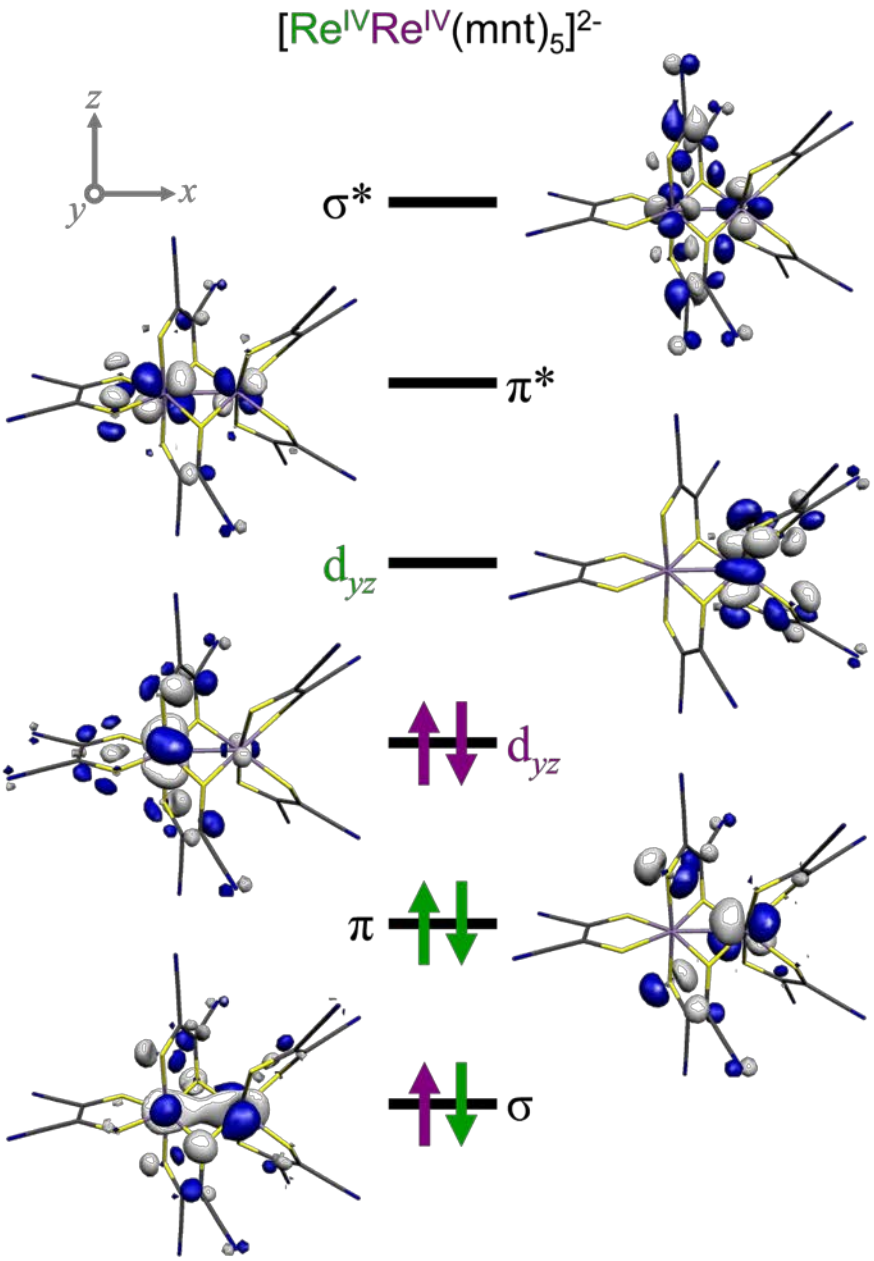

Fig. S7 Qualitative MO scheme depicting the ordering of the frontier orbitals (² -spin) for the $\{Re_2\}^{8+}$ unit in $[Re_2(mnt)_5]^{2-}$.

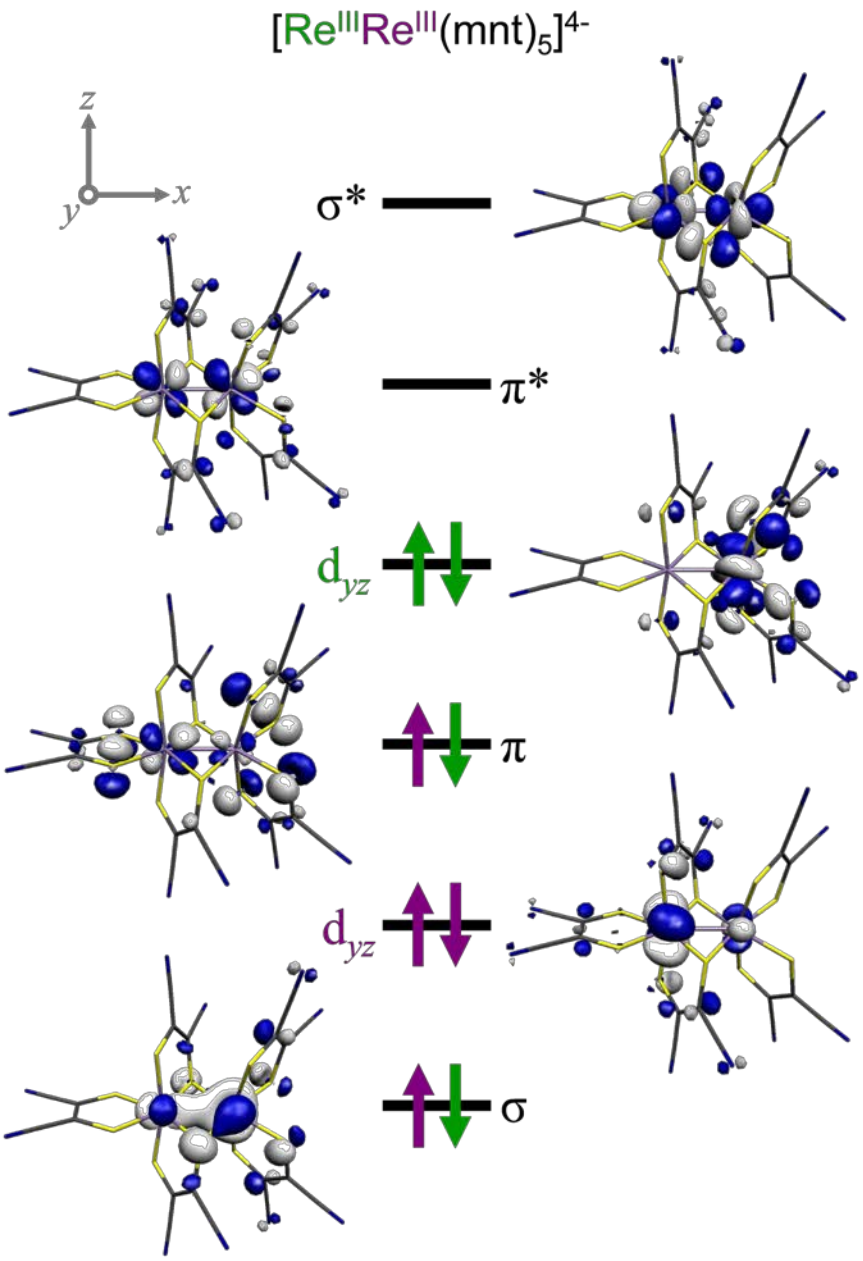

Fig. S8 Qualitative MO scheme depicting the ordering of the frontier orbitals (^{2}-spin) for the $\{Re_2\}^{6+}$ unit in $[Re_2(mnt)_5]^{4-}$.

References

1. A. Davison, R. H. Holm, R. E. Benson and W. Mahler, *Inorg. Synth.*, 1967, **10**, 8.
2. W. L. Amarego and D. D. Perrin, *Purification of Laboratory Chemicals,* 4th edn., Butterworth-Heinemann, Linacre House, Jordan Hill, Oxford, 2000.
3. N. G. Connelly, C. J. Jones and J. A. McCleverty, *J. Chem. Soc. A,* 1971, 712.
4. (a) *APEX2,* Version 2009.3-0, Bruker-AXS Inc., Madison, WI, USA, 2009. (b) *APEX2,* Version 2009.9-0, Bruker-AXS Inc., Madison, WI, USA, 2009.
5. (a) *SAINT,* Version 7.68A, Bruker AXS Inc., Madison, WI, 2009. (b) *SAINT*, Version 7.60A, Bruker AXS Inc., Madison, WI, 2008.
6. Sheldrick, G. M. *SADABS*, Version 2008/2, Universität Göttingen, Göttingen, Germany, 2008.
7. Sheldrick, G. M. *SHELXS-97*, Universität Göttingen, Göttingen, Germany, 2008.
8. Sheldrick, G. M. *SHELXL-97*, Universität Göttingen, Göttingen, Germany, 2008.
9. *SHELXTL*, Version 2008/4, Bruker-AXS, Madison, WI, 2008. (b) *SHELXTL*, Version 6.10, Bruker-AXS, Madison, WI, 2000.
10. See http://checkcif.iucr.org/
11. G. R. Hanson, K. E. Gates, C. J. Noble, M. Griffin, A. Mitchell and S. Benson, *J. Inorg. Biochem.*, 2004, **98**, 903.
12. Neese, F. *Orca, an Ab Initio, Density Functional and Semiempirical Electronic Structure Program Package*, version 3.0; Universität Bonn: Bonn, Germany, 2013.
13. (a) A. D. Becke, *J. Chem. Phys.*, 1993, **98**, 5648. (b) C. T. Lee, W. T. Yang and R. G. Parr, *Phys. Rev. B*, 1988, **37**, 785.
14. F. Weigend and R. Ahlrichs, *Phys. Chem. Chem. Phys.*, 2005, **7**, 3297.

15. (a) E. van Lenthe, J. G. Snijders and E. J. Baerends, *J. Chem. Phys.*, 1996, **105**, 6505. (b) E. van Lenthe, A. van der Avoird and P. E. S. Wormer, *J. Chem. Phys.*, 1998, **108**, 4783. (c) J. H. van Lenthe, S. Faas and J. G. Snijders, *Chem. Phys. Lett.*, 2000, **328**, 107.
16. *Molekel*, Advanced Interactive 3D-Graphics for Molecular Sciences, Swiss National Supercomputing Center. http://www.cscs.ch/molekel